Wear, *151* (1991) 143–156

Monitoring groove wear development in cutting tools via stochastic modelling of three-dimensional vibrations

X. D. Fang, Y. Yao and **G. Arndt**
Department of Mechanical Engineering, University of Wollongong, N.S.W. 2500 (Australia)

(Received April 16, 1991; revised and accepted June 27, 1991)

Abstract

This paper describes an experimental investigation into the patterns of groove wear development and their monitoring at the minor cutting edge of metal-cutting tools. It is shown that these grooves, once formed, adversely affect the dimensional accuracy and surface roughness in finish machining. Multivariate time series stochastic models are developed directly from vibration signals, measured with a miniature three-dimensional (3D) accelerometer mounted in close vicinity to the tool tip. Based on the established models, multiple dispersion analysis is introduced to isolate ingredients sensitive to particular stages of groove wear from the 3D vibrations, and to quantify their relations. The results are physically interpreted and show that the method presented in this paper is a feasible means for on-line monitoring of groove wear development in automated finish machining.

1. Introduction

With the advent of automated machining systems, on-line tool wear estimation plays a vital role in quality assurance, especially for finish machining where the tool change policy is quite different from that under the normal machining conditions. In finish machining, the well-known types of tool wear, such as major flank wear and crater wear, are often not the wear types which lead to tool failure first. Instead, minor flank wear, nose wear and groove wear at the minor cutting edge are recognized as being more important in determining the tool life, because of their greater influence on the dimensional accuracy and surface quality of the finished product [1]. In particular, groove wear at the minor cutting edge, once formed, will cause significant deterioration of surface quality and shorten tool life.

Much work has been reported on tool wear estimation, as described in several survey papers [2–6]. However, almost all of them were concerned with the common types of wear, *i.e.* major flank wear and crater wear. In our recent work [7], an approach to comprehensive tool wear estimation (including minor flank wear) was presented based on multivariate time series analysis.

The study of groove wear at the minor cutting edge can be dated back to the 1960s [8–14]. Most work then focused on explaining the phenomena and conjecturing the mechanism of formation. The formation of the groove is mainly due to the rubbing action at the minor cutting edge from a mechanical point of view. The workpiece, with a work-hardened layer, can be compared with a grinding wheel. Groove wear

0043-1648/91/$3.50

will occur under certain combinations of tool and work materials, and it can be observed that a series of grooves will form at the minor cutting edge which in fact does not take part in cutting directly. The depth of groove wear directly influences the surface roughness produced. Shown in Fig. 1 is a pictorial description of the groove wear at the minor cutting edge in accordance with CIRP terminology [1]. It was found that, when enough grooves have been formed and developed to a certain degree, severe vibration may be induced, which disturbs the formed groove pattern and wipes out the grooves eventually, resulting in a rapid deterioration of surface finish [12]. In other words, groove wear reaches its critical point and the cutting tool should be replaced when the grooves are being wiped out.

Although vibrations induced by groove wear at the minor cutting edge have been observed long ago [8], no further work has been reported on investigating the possibility of using it for on-line monitoring purposes, mainly because of the complexity involved in groove wear formation and the difficulty involved in effective signal analysis and interpretation. The study of on-line groove wear monitoring, however, is of significance in automated machining systems, not just because of its influence on surface quality, but also because groove wear is often one of the factors inducing unfavourable chatter [11]. Although it was reported that superimposing a minor vibration in the feed direction hindered groove formation [11, 12], this is not economically justifiable for conventional machine tool structures.

The purpose of this work is to develop an effective method to detect and monitor the formation and development of groove wear. The paper first presents the experimental results of groove wear development and investigation results concerning the detection of the critical point at which severe vibration is induced by the groove wear, *i.e.* at which the finishing tool needs to be replaced. Because vibration occurring in the neighbourhood of that point in time is extremely complicated and because very little is known about it, a miniature three-dimensional (3D) accelerometer, mounted in the close vicinity of the tool tip, was used to capture multidimensional vibration signals. Since more than one quantity is needed to describe the groove wear, and the formation of groove wear is related to all three orthogonal cutting directions, multivariate autoregressive (ARV) time series models are adopted. Based on stochastic ARV models developed directly from the vibration signals, a quantitative analysis was made possible by employing multiple-dispersion analysis, which discriminates features which are sensitive to various aspects of the formation of groove wear.

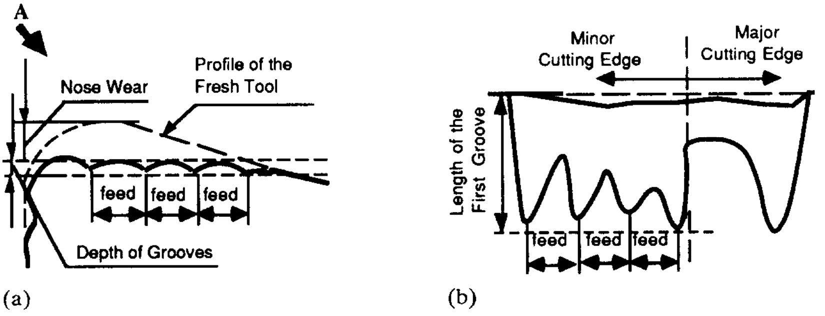

(a) (b)

Fig. 1. Groove wear at the minor cutting edge: (a) view from tool top face; (b) view from A.

2. Investigation into the patterns of groove wear development

2.1. Tool wear experiments

In the experiments, 3D vibration signals were measured with a miniature 3D accelerometer (PCB model 306A06), mounted in the close vicinity of the tool tip, aiming at capturing original signals with minimum distortion. The machining conditions used in the experiments are shown in Table 1, all the conditions being within the range recommended by the tool manufacturer.

The machining process was interrupted periodically in order to measure tool wear and surface roughness. Two sets of 524 data points each, one with a sample interval of 30 μs and the other 3.13 ms, were taken from the vibration signal in each of the three orthogonal directions, just before each interruption. An extra two sets of data were also recorded between consecutive interruptions to provide more information for signal processing.

2.2. Development of groove wear

In order to describe quantitatively the development of groove wear at the minor cutting edge, four parameters were selected: the number of grooves at the minor cutting edge, the depth of the grooves, the maximum groove length (defined as the maximum length of any groove measured downwards from the minor cutting edge), and the groove wear area (defined as the product of the maximum groove length and the distance between the first and the last grooves on the minor flank). Nose wear was also selected because of its relevance to groove wear. Figures 2–6 show the measurement results of these wear parameters under all five cutting conditions. The surface roughness was plotted in Fig. 7.

2.3. Patterns of groove wear development

From an analysis of the above figures, it is seen that two different groove wear patterns can be identified, one for the lower feed (0.04 mm rev^{-1}), designated as groups B and E, and the other for higher feed (0.08 mm rev^{-1}), designated as groups A, C and D. For the lower feed, it can be seen the number of grooves decreases at a certain point (Fig. 2) and the surface finish deteriorates sharply at the same time (Fig. 7). It is evident that the wipe-out of grooves causes the deterioration. It is also seen that the depths of grooves fluctuates for the low feed group B (Fig. 3) because of the concurrence of the formation of new grooves and the wipe-out of formed grooves, while for the higher feed no decrease in the number of grooves nor a sharp increase in surface roughness are observed, even after machining for over 45 min

TABLE 1

Machining conditions used in groove wear experiments

Machine tool	HITEC-20SII CNC Lathe (18 kW)
Tool insert type	TNMG 160408 (Carbide P10)
Tool geometry	0°, 5°, −6°, 90°, 60°, 0.8
Work material	AISI4140 (Brunell hardness, 320)
Cutting conditions	
Group A	V=160 m min^{-1}, f=0.08 mm rev^{-1}, d=0.25 mm
Group B	V=160 m min^{-1}, f=0.04 mm rev^{-1}, d=0.25 mm
Group C	V=125 m min^{-1}, f=0.08 mm rev^{-1}, d=0.25 mm
Group D	V=190 m min^{-1}, f=0.08 mm rev^{-1}, d=0.25 mm
Group E	V=190 m min^{-1}, f=0.04 mm rev^{-1}, d=0.25 mm

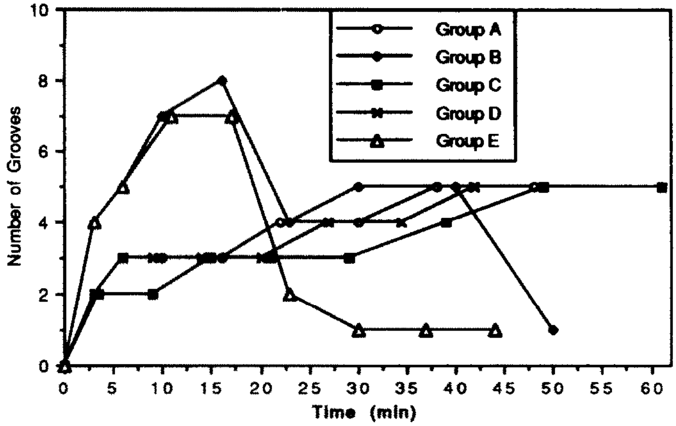

Fig. 2. Number of grooves at the minor cutting edge.

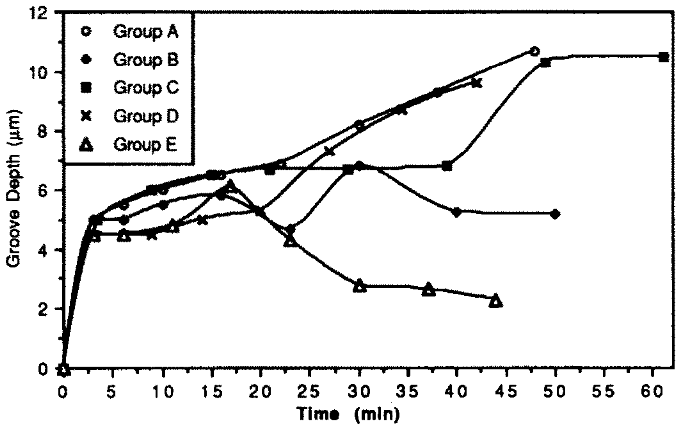

Fig. 3. Development of groove depth.

Fig. 2). This may be because the higher feed rate results in wider ridges between adjacent grooves, and thus in better wear resistance. It is consistently observed for all five cutting conditions that, when the groove wear at the minor cutting edge has developed to a point at which tool failure is indicated, the major flank wear is still far below its critical value. Therefore it can be concluded that the groove wear, once formed at the minor cutting edge, will largely dictate the tool life in finish machining. Scanning electron microscopy (SEM) was used for a more detailed analysis, with some results being shown in Figs. 8 and 9.

2.3.1. Lower feed (groups B and E)

Four typical stages are found under the lower feed condition, as shown in Fig. 8.

(a) *Initial stage*. Before the grooves are formed, the surface roughness is mainly determined by the tool geometry of the fresh tool as well as the cutting conditions used, usually representing the best possible surface roughness condition in finish machining.

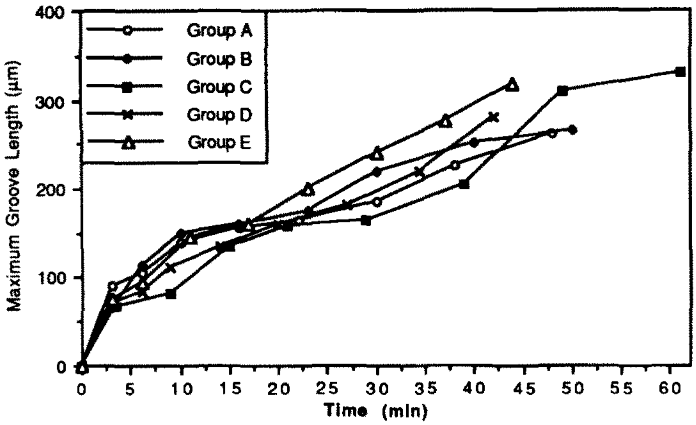

Fig. 4. Development of maximum groove length.

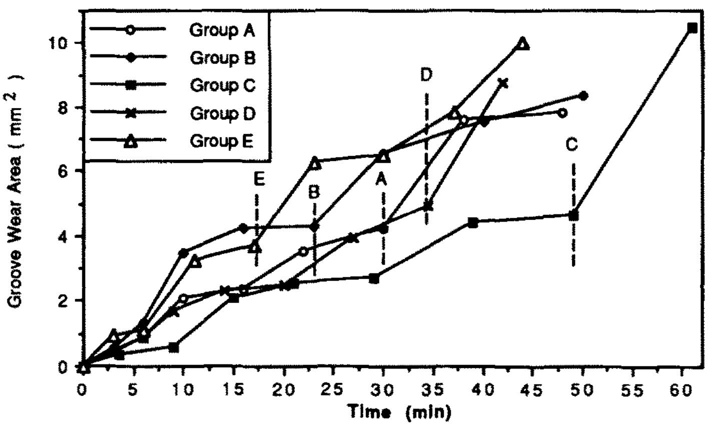

Fig. 5. Development of groove wear area.

(b) *Steady stage*. In the next few minutes, the grooves will form at the minor cutting edge under certain machining conditions. Once these grooves are formed, the surface roughness will increase and largely depend on the depth of the grooves. As the depth of grooves develops slowly during this period, the surface roughness remains constant.

(c) *Severe stage*. From Fig. 8(c), it is clear that at this stage the grooves are being wiped out because of the induced vibration. When the regular groove pattern is disturbed, the surface roughness increases sharply, resulting in a very poor surface quality.

(d) *Disappearing stage*. At this stage, most grooves have been wiped out and the minor flank face is left in a very rough condition and loses its function as a finishing tool.

2.3.2. Higher feed (groups A, C and D)

For the higher feed, no decrease in the number of grooves occurs and three typical stages as shown in Fig. 9 may be identified.

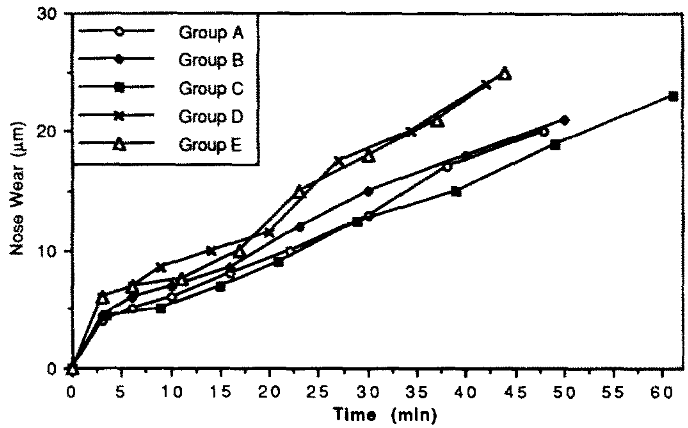

Fig. 6. Development of nose wear.

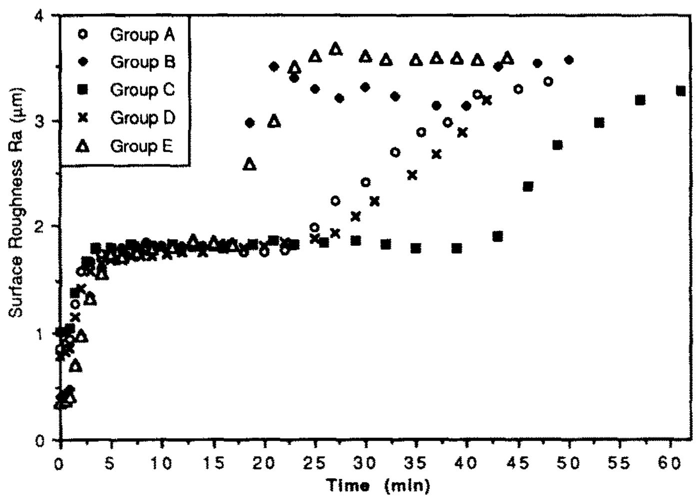

Fig. 7. Surface roughness for five cutting conditions.

(a) *Initial stage*. At this stage, groove wear development is similar to that under the lower feed, while the surface finish is poorer owing to the higher feed used.

(b) *Steady stage*. There seems to be no significant difference in surface roughness compared with the lower feed group. However, the grooves formed at the minor cutting edge are fewer owing to the high feed used.

(c) *Accelerating stage*. Shown in Fig. 9(c) is the accelerating stage of groove wear, during which the surface roughness (Fig. 7) begins to increase quickly and soon becomes unsuitable for finish machining. Viewed together with Fig. 5, which shows the development of groove wear area, it is found that the starting point of rapid deterioration of surface finish always corresponds to the beginning of acceleration of the groove wear area, indicated by the broken vertical lines in Fig. 5. Therefore it is conjectured that the rapid increase of surface roughness at the high feed is due to the larger contact area between the tool minor flank and the machined workpiece surface.

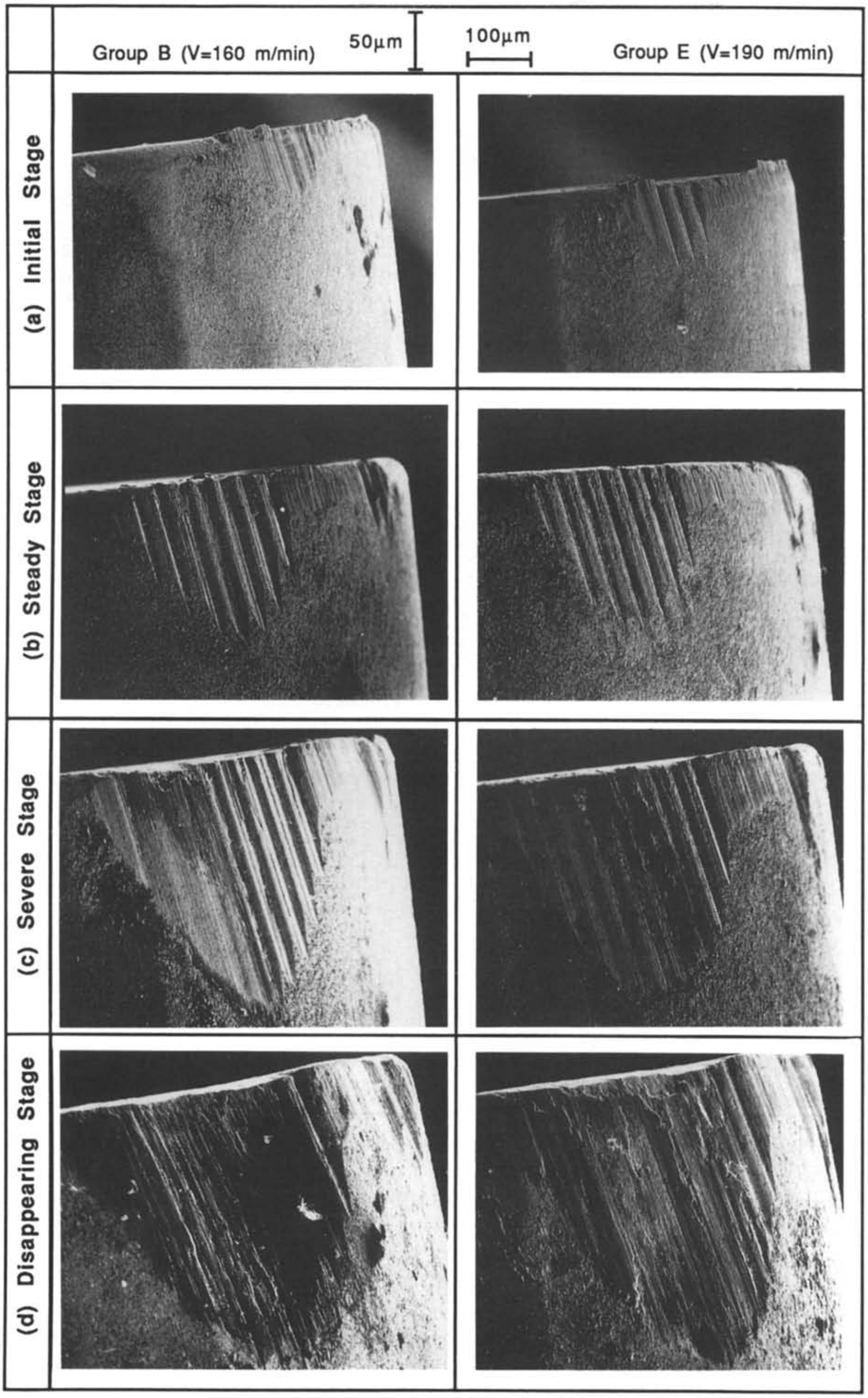

Fig. 8. Groove wear development under the lower feed condition (0.04 mm rev^{-1}).

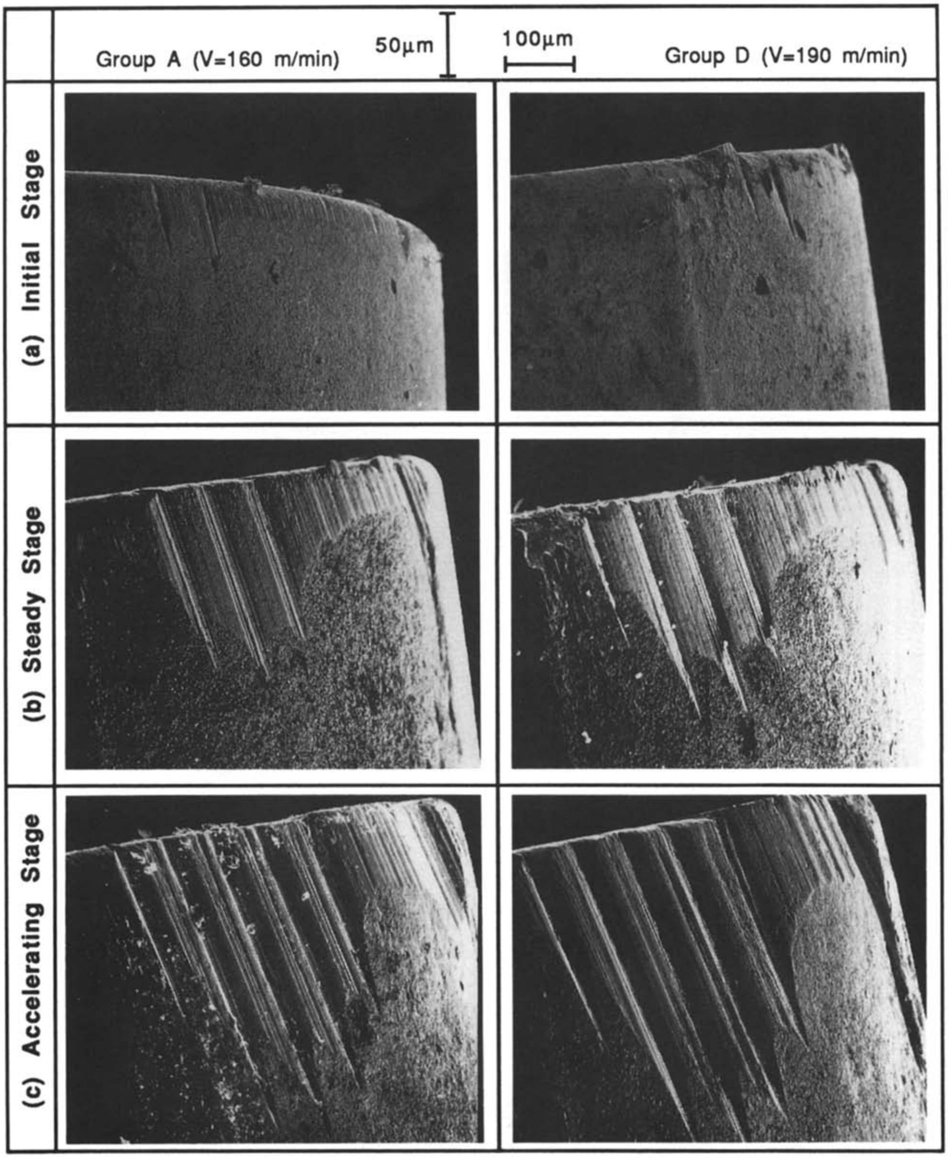

Fig. 9. Groove wear development under the higher feed condition (0.08 mm rev^{-1}).

3. Stochastic modelling of three-dimensional vibrations

3.1. Application of autoregressive vector time series modelling

Autoregressive vector time series models were developed to quantify statistically the dynamics embedded in the 3D vibration data. The merit of employing such a technique lies in the fact that it provides a mathematical model primarily based on the observed data and does not require much prior knowledge or assumptions about the underlying system dynamics. The vibration signals, recorded in three orthogonal directions and sampled at uniform intervals, can be represented in the form of vector difference equations, *i.e.* either in the explicit Green's function or in a stochastic ARV(n) model with autoregressive order n

$$X_t = \sum_{k=0}^{\infty} \mathbf{G}_k \boldsymbol{a}_{t-k} \qquad \text{or } X_t = \sum_{k=1}^{n} \boldsymbol{\Phi}_k X_{t-k} + \boldsymbol{a}_t \tag{1}$$

where

$$X_t = [X_{1t}, X_{2t}, X_{3t}]^{\mathrm{T}}$$

$$\boldsymbol{\Phi}_k = \begin{bmatrix} \Phi_{11k} & \Phi_{12k} & \Phi_{13k} \\ \Phi_{21k} & \Phi_{22k} & \Phi_{23k} \\ \Phi_{31k} & \Phi_{32k} & \Phi_{33k} \end{bmatrix}$$

$$\boldsymbol{a}_t = [a_{1t}, a_{2t}, a_{3t}]^{\mathrm{T}}$$

In this way, the observed trivariate series, $X_{1t} = V_{xt}$ equal to vibration in the feed direction, $X_{2t} = V_{yt}$ equal to vibration in the thrust direction, and $X_{3t} = V_{zt}$ equal to vibration in the main cutting direction, are expressed as linear combinations of past observation vectors $t-k$ in terms of autoregressive parameter matrices $\boldsymbol{\Phi}_k$ ($k = 1, 2, \ldots, n$) plus an independent random vector $\boldsymbol{a}_t$ and therefore describe the instantaneous dynamics of the cutting process.

3.2. Multiple-dispersion analysis

Dispersion analysis provides an effective means for quantitative model decomposition in order to identify particular variations convolved in the recorded data [7, 15–17]. As the formation of groove wear stems from complex interactions among all 3D vibrations and much about it is still not clear, multiple-dispersion analysis is used to quantify not only the contribution of individual variables but also the interactions among different variables. Using the explicit Green's function of eqn. (1), the vector autocovariance matrix γ_0 can be determined as follows

$$\gamma_0 = E[X_t X_t^{\mathrm{T}}] = \sum_{k=0}^{\infty} \mathbf{G}_k \boldsymbol{\sigma}_a^2 \bar{\mathbf{G}}_k^{\mathrm{T}} \tag{2}$$

where $\boldsymbol{\sigma}_a^2$ is the residual matrix and $\bar{\mathbf{G}}_k$ is the complex conjugate of $\mathbf{G}_k$. It has been shown that the explicit Green's function can be obtained from the established ARV(n) model under the assumption of distinct eigenvalues [18] as follows

$$\mathbf{G}_k = \sum_{i=1}^{n} \mathbf{T}_i \boldsymbol{\lambda}_i^{k+n-1} \mathbf{U}^{-1} \mathbf{U}_i \mathbf{T}_i^{-1} \tag{3}$$

where

$$\mathbf{U} = \prod_{i,j=1 \text{ and } i>j}^{n} (\boldsymbol{\lambda}_i - \boldsymbol{\lambda}_j)$$

and

$$\mathbf{U}_i = (-1)^i \prod_{i,j=1 \text{ and } i>j \text{ and } i,\, j\neq k}^{n} (\boldsymbol{\lambda}_i - \boldsymbol{\lambda}_j)$$

The eigenvalue matrices $\boldsymbol{\lambda}_i = \mathrm{diag}[\lambda_{xi}, \lambda_{yi}, \lambda_{zi}]$ and eigenvector matrix $\mathbf{T}_i$, $i = 1, \ldots, n$, are found by adjoining the parameter matrices $\boldsymbol{\Phi}_k$ of the ARV(n) model, and finally the following form of the equation for a symmetric vector autocovariance matrix γ_0 can be derived:

$$\gamma_0=\begin{bmatrix}\gamma_{0xx} & \gamma_{0xy} & \gamma_{0xz}\\ & \gamma_{0yy} & \gamma_{0yz}\\ & & \gamma_{0zz}\end{bmatrix}=\begin{bmatrix}\sum_{i=1}^{n}\sum_{j=1}^{n}D_{ixxj} & \sum_{i=1}^{n}\sum_{j=1}^{n}D_{ixyj} & \sum_{i=1}^{n}\sum_{j=1}^{n}D_{ixzj}\\ & \sum_{i=1}^{n}\sum_{j=i}^{n}D_{iyyj} & \sum_{i=1}^{n}\sum_{j=1}^{n}D_{iyzj}\\ & & \sum_{i=1}^{n}\sum_{j=1}^{n}D_{izzj}\end{bmatrix} \tag{4}$$

Thus the vector autocovariance of the entire process is decomposed into the contributions of process eigenvalues as well as the complex interactions between various eigenvalues in terms of multiple dispersion D_{ixxj}, D_{ixyj} etc. Of particular interest are the multiple dispersions corresponding to the complex eigenvalues which reflect the oscillating characteristics of the machining process. The characteristic frequency f_n corresponding to a pair of underdamped complex conjugate roots λ_1 and λ_2 can be determined by the following equation [16]

$$f_n(\mathrm{Hz})=\frac{1}{2\pi\Delta}\left(\frac{\{\ln(\lambda_1\lambda_2)\}^2}{4}+\left[\cos^{-1}\left\{\frac{\lambda_1+\lambda_2}{2(\lambda_1\lambda_2)^{1/2}}\right\}\right]^2\right)^{1/2} \tag{5}$$

where Δ is the sampling interval.

4. Strategy for groove wear monitoring by multiple-dispersion analysis

The 3D vibration signals were modelled as a stochastic ARV(n) model. The multivariate time series analysis and the results of multiple-dispersion analysis are presented below in relation to the detection and monitoring of groove wear development.

4.1. Groove wear monitoring for the lower feed condition

Three distinctive dispersions were found as being related to the development of groove wear, as shown in Fig. 10 for group B as a representative of the lower feed condition (0.04 mm rev^{-1}). The first two patterns are associated with high frequency dispersions. One is the dispersion in the thrust direction D_{yy} at around 9.3 kHz and another is that in the main cutting direction D_{zz} at around 2.5 kHz. It was found that, when the number of grooves decreased from the value at 16 min to the value at 23 min (Fig. 2), D_{yy} and D_{zz} reached their maximum value, signifying the severe vibration occurring under these frequencies. The third pattern is the cross-dispersion D_{yz} in the low frequency range between the vibrations in the thrust direction at 150 Hz and the main cutting direction at 145 Hz (Fig. 10). The moment at which D_{yz} reaches its peak value also matches that when the number of grooves decreases and the roughness deteriorates rapidly. If one compares the times of peak dispersions, it is seen that D_{yy} occurred at about 19 min and D_{zz} and D_{yz} at about 22 min. This may indicate that vibration is first induced in the thrust direction which disturbs the regular grooves formed. The disturbed minor cutting edge in turn excites vibration in the main cutting direction. Therefore the following criterion can be established: the peak

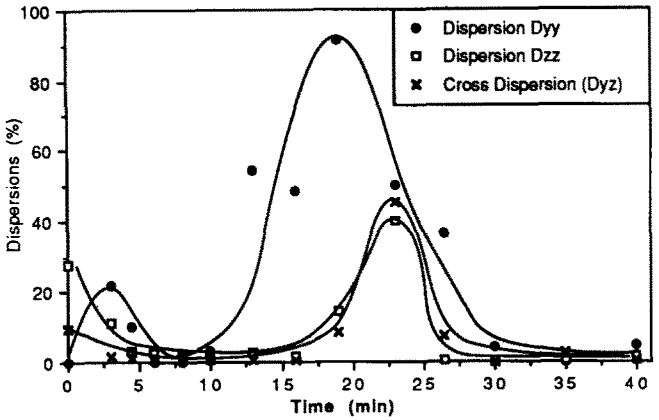

Fig. 10. Dispersion patterns for the lower feed condition (0.04 mm rev^{-1}).

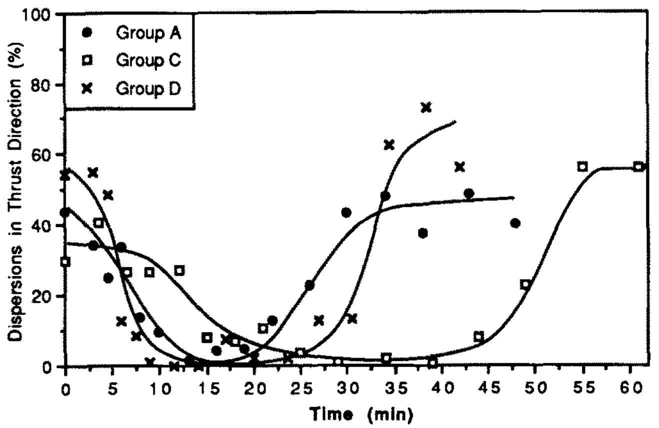

Fig. 11. Dispersion patterns for the higher feed condition (0.08 mm rev^{-1}).

value of D_{yy} indicates the commencement of groove wipe-out, while that of D_{zz} and D_{yz} indicates the ending of groove wipe-out. This criterion can be used in finish machining to determine the necessity of tool replacement for the lower feed condition.

4.2. Groove wear monitoring for the higher feed condition

For this condition, the dispersion pattern found is totally different from that for the lower feed, because of the difference in groove wear development. A clear concave trend shown in Fig. 11 was found for the dispersion in the thrust direction, with the frequency equal to about 9.4 kHz. By comparing the surface roughness development (Fig. 7) with the above dispersion pattern, it is seen that consistency exists between them, as summarized in Table 2.

From the analysis in Table 2, it can be concluded that the behaviour of the dispersion in the thrust direction (9.4 kHz), isolated from the 3D vibration variations, resembles the rate (slope) of the surface roughness development shown in Fig. 7. Thus this dispersion could be used as an index for the severity of the groove wear at the minor cutting edge under higher feed conditions.

TABLE 2

Relationship between surface roughness and dispersion pattern

Groove wear development	Changes in surface roughness for the higher feed group	Dispersion pattern around the natural frequency of tool–tool holder assembly
Initial stage	Increasing rapidly owing to the normal tool running-in	Appearing in high values during the tool running-in period
Steady stage	Remaining constant as the groove depth develops slowly	Decreasing to the minimum owing to the smaller variations involved in the thrust vibration signals
Accelerating stage	Starting to accelerate owing to the severity of groove wear indicated by the acceleration of groove wear area (Fig. 5)	Increasing to a high value again owing to the changes in thrust vibration caused by the severe groove wear

5. Physical interpretations

Clear patterns have been identified relating the vibration in terms of multiple dispersions and corresponding frequencies to the different stages of groove wear development. For the lower feed condition (0.04 mm rev^{-1}), more grooves are formed and earlier vibration is induced, giving rise to a worse surface finish, while the higher feed condition (0.08 mm rev^{-1}) appears to have a better wear resistance. The difference between the lower and higher feed conditions lies in the fact that, for a selected tool geometry, the feed becomes a dominant factor to determine the grooves' spacing at the minor cutting edge. It is noticed that, in the case where grooves are formed, the lower feed condition does not produce a better surface finish.

For both conditions the dispersion analysis results, based on the stochastic model developed from the experimental data directly, indicate that groove wear development finds its reflection mainly in the thrust vibration. This can be explained as follows. This vibration, *i.e.* the relative displacement between the workpiece and the tool tip in the radial direction, is a compound effect of the workpiece lateral dynamics and the tool–tool holder dynamics. In the analysis for the lower feed condition it was shown that the dispersions of the thrust vibration reached their peaks at about 150 Hz and 9300 Hz respectively, with the higher peak dominant when the number of grooves began to decrease, *i.e.* the surface roughness began to deteriorate rapidly. These frequencies, as expected, correspond to the natural frequencies of the workpiece and tool–tool holder assembly, which were determined to be around 155 Hz and 9340 Hz respectively using conventional excitation tests. These close agreements may indicate that, when a sufficient number of grooves have been formed, the dynamics of the cutting process is excited, so that more severe vibration at the characteristic frequencies is induced. Similar results were obtained in the dispersion analysis of vibration in the main cutting direction. For the high feed condition, the dispersions in the thrust direction around the natural frequency of tool–tool holder assembly were again found to be closely related to the surface roughness development determined by the severity of groove wear at the minor cutting edge. Tables 3 and 4 summarize these physical interrelationships.

TABLE 3

Comparison between dispersion analysis results and physical quantities for the lower feed (0.04 mm rev^{-1})

Vibration direction	Peak frequency (Hz) detected using the dispersion analysis when the number of grooves began to decrease		Natural frequency (Hz) determined by using conventional excitation tests	
	In the range of low frequencies	In the range of high frequencies	Workpiece system	Tool–tool holder assembly
Thrust	150	9300	155	9340
Main cutting	145	2500	155	2610

TABLE 4

Comparison between dispersion analysis results and physical quantities for the higher feed (0.08 mm rev^{-1})

	Characteristic frequency (Hz) of dispersion which resembles the rate of surface roughness	Natural frequency (Hz) of the tool–tool holder assembly
Thrust vibration	9400	9340

6. Conclusions

(1) The purpose of this work was to investigate the relationships between off-line measurements of groove wear at the minor cutting edge and multiple-dispersion analysis based on the stochastic modelling of 3D vibration in finish machining, such that the latter alone will be capable of on-line monitoring of groove wear development at the minor cutting edge.

(2) The development patterns of groove wear at the minor cutting edge and the associated surface roughness were investigated under typical cutting conditions. It was found that if a finish-machining condition under which grooves will form at the minor cutting edge is used, the feed is the dominant factor in determining the development patterns of groove wear.

(3) Multiple-dispersion analysis of the 3D vibration has been proven to be effective in detecting the critical points at which either the surface finish deteriorates sharply owing to the wiping-out of grooves at the minor cutting edge, or the acceleration of surface roughness induced by the rapid increase in groove wear area occurs. The criteria derived from the dispersion analysis are all based on the frequencies which can be physically interpreted. Although these frequencies may vary for different workpiece geometries and tool–tool holder assemblies, they are not difficult to determine.

(4) The results of this work further emphasize that groove wear at the minor cutting edge may occur during finish machining under a fairly wide range of cutting conditions for the commonly used cutting tool and work materials. Should grooves be formed, the life of the finishing tool will be significantly shortened.

(5) The monitoring method presented in this paper offers one avenue by which surface finish may be controlled in automated finish machining, as an essential component of product quality assurance.

Acknowledgment

The authors gratefully acknowledge partial support from the Australian Research Council.

References

1 A. J. Pekelharing and C. A. Van Luttervelt, *CIRP Terminology and Procedures for Turning Research.*, Technical Secretary CIRP group C, Delft, 1969.
2 J. Tlusty, A critical review of sensors for unmanned machining, *Ann. CIRP, 32* (2) (1983) 563–572.
3 H. K. Toenshoff, J. P. Wulfsberg, H. J. J. Kals and W. Koenig, Developments and trends in monitoring and control of machining processes, *Ann. CIRP, 37* (2) (1988) 611–622.
4 L. Monostori, Signal processing and decision making in machine tool monitoring systems, *Proc. 16th N. Amer. Manuf. Research Soc. Conf.,* Society of Manufacturing Engineers, Urbana, IL, 1988, pp. 277–284.
5 M. Shiraishi, Scope of in-process measurement, monitoring and control techniques in machining processes — Part 1: In-process techniques for tools, *Precis. Eng., 10* (4) (1988) 179–189.
6 D. Li and J. Mathew, Tool wear and failure monitoring techniques for turning — a review, *Int. J. Mach. Tools Manuf., 30* (4) (1990) 579–598.
7 Y. Yao, X. D. Fang and G. Arndt, Comprehensive tool wear estimation in finish-machining via multivariate time-series analysis of 3-D cutting forces, *Ann. CIRP, 39* (1) (1990) 57–60.
8 A. J. Pekelharing and R. A. Schuermann, Wear of carbide tools — its effect of surface finish and dimensional accuracy, *Tool Eng., 30,* (October 1953) 51–57.
9 V. Solaja, Wear of carbide tools and surface finish generated in finish turning of steel, *Wear, 2* (1958–1959) 40–58.
10 A. J. Pekelharing, Finish turning, *Ann. CIRP, 8* (1959) 112–120.
11 B. H. Lambert, Two years of finish-turning research at the Technological University, Delft, *Ann. CIRP, 10* (1961–1962) 246–255.
12 A. J. Pekelharing, Some special aspects of carbide tool wear, Proc. Int. Production Engineering Research Conf., Pittsburgh, 1963, ASME, New York, 1963.
13 M. C. Shaw and J. A. Crowell, Finish machining, *Ann. CIRP, 13* (1965) 5–22.
14 A. J. Pekelharing and H. J. Hovinga, Wear at the end cutting edge of carbide tools in finish and rough turning, *Proc. 8th Int. Machine Tool Design and Research Conf.,* Pergamon, Manchester, 1967, pp. 643–651.
15 W. R. DeVries, D. A. Dornfeld and S. M. Wu, Bivariate time series analysis of the effective force variation and friction coefficient distribution in wood grinding, *J. Eng. Ind., 100* (1978) 181–185.
16 S. M. Pandit and S. M. Wu, *Time Series and System Analysis with Applications,* Wiley, New York, 1983.
17 K. Eman and S. M. Wu, A feasibility study of on-line identification of chatter in turning operations, *J. Eng. Ind., 102* (1980) 315–321.
18 S. M. Pandit, Data dependent systems: modeling analysis and optimal control via time series, *Ph.D. Thesis,* University of Wisconsin, Madison, WI, 1973.